buckling load (provided the resultant compressive forces act at the ring centerline) with

$$I_2 = \pi r^3 \tag{27}$$

$$J = 2\pi r^3 \tag{28}$$

Then, from Eqs. (23), (5), (25), and (26),

$$N_c R + \frac{9\pi E r^3 (pr + G_o)(pr + 2G_o)}{R^2(pr + G_o)(4pr + 8G_o + E) + 9Er^2(pr + 2G_o)} \tag{29}$$

If the skirt tension resultant does not pass through the center of the ring cross section (as in Fig. 1), uniformly distributed couples exist around the ring, which result in a bending moment that affects the critical buckling load. A combined bending-compression buckling is, however, beyond the scope of this paper. The equations for buckling of cones or noncircular toroids are different, but the approach is similar.

References

[1] Topping, A. D., "Shear Deflections and Buckling Characteristics of Inflated Members," *Journal of Aircraft*, Vol. 1, No. 5, Sept.–Oct. 1964, pp. 289–292.

[2] Topping, A. D., "An Introduction to Biaxial Stress Problems in Fabric Structures," *Aerospace Engineering*, Vol. 20, No. 4, April 1961; pp. 18–19, 53–57.

[3] Leonard, R. W., Brooks, G. W., and McComb, H. G., "Structural Considerations of Inflatable Re-entry Vehicles," TN D-457, Sept. 1960, NASA.

[4] Leonard, R. W., McComb, H. G., Zender, G. W., and Stroud, W. J., "Analysis of Inflated Re-entry and Space Structures," *Symposium on Recovery of Space Vehicles*, Los Angeles Section of The Institute of Aeronautical Sciences, Los Angeles, Calif., Aug. 31–Sept. 1, 1960.

[5] Timoshenko, S. and Gere, J. M., "Theory of Elastic Stability," 2nd ed., McGraw-Hill, New York, 1961, pp. 132–135.

[6] Shanley, F. R., "Weight-Strength Analysis of Aircraft Structures," 2nd ed., Dover, New York, 1960, pp. 323–342.

[7] Foerster, A. F. et al., "Analytical and Experimental Investigation of Coated Metal Fabric Expandable Structures for Aerospace Applications," ASD-TDR-63-542, Aug. 1963.

[8] Seide, P., Weingarten, V. I., and Morgan, E. J., "Final Report on the Development of Design Criteria for Elastic Stability of Thin Shell Structures," AFBMF/TR-61-7, Dec. 31, 1960.

[9] Nicolai, E. L., "Stability Problems in Theory of Elasticity," *Zeitschrift fur Angewandte Mathematik and Mechanik*, Vol. 3, 1923, pp. 227–229.

[10] Topping, A. D., "Buckling Resistance of Inflated Cylinders in Bending," *Transactions of the Third Aerospace Expandable and Modular Structures Conference*, AF APL TR 68-17, 1967, pp. 147–165.

NOVEMBER 1971 J. AIRCRAFT VOL. 8, NO. 11

Airfoils in Two-Dimensional Nonuniformly Sheared Slipstreams

G. R. Ludwig* and J. C. Erickson Jr.†
Cornell Aeronautical Laboratory Inc., Buffalo, N. Y.

A theoretical and experimental program has been conducted to investigate the aerodynamics of an airfoil in a two-dimensional nonuniformly sheared slipstream. A mathematical model has been developed to predict airfoil pressure distributions in such a slipstream and has been used successfully for slipstreams with moderate shear. Pressure distributions over a wide angle-of-attack range have been measured experimentally on an airfoil at each of seven different locations in a highly sheared two-dimensional slipstream. Study of the pressure distributions obtained on the airfoil at a location slightly above the flow centerline and also at a location slightly below the flow centerline indicates that the large effects on stalling characteristics are due to differences in the upper surface pressure distributions. These pressure distributions are affected by the freestream shear. Moreover, in the data obtained for airfoils located near the flow centerline, the differences in the lift appear to be caused primarily by differences in the stagnation pressure of the streamline which intersects the airfoil. This stagnation pressure is a function not only of airfoil location relative to the slipstream, but also of the angle of attack of the airfoil.

Nomenclature

c = airfoil chord, Fig. 1a
C_l = sectional lift coefficient
C_p = pressure coefficient
h = vertical height of airfoil midchord above tunnel centerline, Fig. 1
L = vertical distance from tunnel centerline to tunnel floor or ceiling, Fig. 1a
r = vertical distance from tunnel centerline to point of maximum velocity in undisturbed nonuniformly sheared slipstream profile, Fig. 1b
x = coordinate along axis parallel to tunnel floor and ceiling, positive downstream; $x = 0$ at airfoil leading edge
y = coordinate perpendicular to x axis, positive upward; $y = 0$ at tunnel centerline
α = airfoil angle of attack, positive leading edge up, Fig. 1
ψ = stream function, Eq. (1)
$(\ )_R$ = coefficient referred to freestream velocity at airfoil midchord position
$(\ )_S$ = coefficient referred to freestream velocity along airfoil stagnation streamline

Presented as Paper 71-94 at the AIAA 9th Aerospace Sciences Meeting, New York, January 25–27, 1971; submitted February 8, 1971; revision received July 23, 1971. This research was supported by the U.S. Army Research Office-Durham on Contract DAHC04-67-C-0071. The authors wish to acknowledge the contributions of W. G. Brady to the theoretical investigation and of J. Nemeth Jr., to the performance of the experiments.

Index categories: Rotary Wing and VTOL Aerodynamics; Jets, Wakes and Viscid-Inviscid Flow Interactions.

* Principal Aeronautical Engineer. Member AIAA.
† Research Aeronautical Engineer. Member AIAA.

Introduction

THE majority of aerodynamic problems are concerned with the determination of forces on bodies immersed in a uniform stream. There are, however, situations in which the flow approaching the body cannot be considered uniform. For example, the flow in propeller or jet slipstreams, in the wakes of bodies, and in boundary layers (including that generated in the atmosphere near the ground) fall into the category of sheared flows. Each of these flows has velocity gradients or shears which vary in magnitude depending on the particular configuration. The theory of sheared or rotational flows is a much more difficult discipline than that of irrotational flows. Useful results have been obtained in only a few very special cases. However, the importance of some of the problems in which sheared flows occur has led to a continued interest in this subject.

The present investigation is the most recent in a systematic study[1-5] of the aerodynamics of airfoils in sheared flows. The studies were initiated as part of a general examination of problems associated with low-speed flight. Attention was focused subsequently on sheared flows because of their importance to rotor or propeller slipstream interaction with the wings of V/STOL aircraft. The investigations have included both theoretical and experimental investigations of airfoils in various types of sheared flows in which the shear exists in a plane perpendicular to the span of the wing.

In the earliest work, Sowyrda[1] extended Tsien's theory[6] for a symmetric Joukowski airfoil in a two-dimensional uniformly sheared stream (i.e., with constant shear throughout the flow) to the case of a cambered Joukowski airfoil. Next, an experimental study was undertaken[2] in which measurements were made on a symmetric two-dimensional Joukowski airfoil. A Joukowski airfoil section was chosen so that the results could be compared to the predictions of the theories available at the time.[1,6-8] One particularly notable result was obtained[2] when the airfoil was immersed in a nonuniformly sheared flow similar to a section through a propeller slipstream. It was found that the location of the airfoil in this flow had a marked effect on both the maximum lift available and on the stalling characteristics of the airfoil. Indeed, it was observed that a small change in the vertical location of the airfoil relative to the flow centerline, say, of approximately one airfoil thickness, produced about a 100% change in maximum lift available. The theories available at the time did not provide a satisfactory explanation for the flow mechanism involved in producing such a marked effect.

A symmetrical Joukowski airfoil was also tested experimentally in an axisymmetric nonuniformly sheared slipstream.[3-4] The results suggested that the sectional aerodynamic moment and lift characteristics inside an axially symmetric slipstream are similar to those obtained in a two-dimensional flow with a similar sheared freestream velocity distribution, provided that the portion of the wing outside the slipstream remains unstalled. This suggested that knowledge of the aerodynamic properties of airfoil sections in two-dimensional flow is of principal importance for the solution of the three-dimensional problem. Therefore, in subsequent studies attention has been concentrated on two-dimensional sheared flows.

An investigation was undertaken next to examine the reason for the sensitivity of airfoil aerodynamic behavior to its location in a nonuniformly sheared slipstream. This was carried out by Brady and Ludwig[5] who treated the symmetric Joukowski airfoil in a nonuniformly sheared flow profile which was kept as simple as possible, see Fig. 1a. The pressure distributions on the airfoil were measured experimentally and compared to the predictions of a theory which was also developed during the program. In principle, the theory is applicable to a freestream velocity profile which can be represented by piecewise linear segments such as those shown in Fig. 1. The theory requires the use of a digital computer to obtain solutions. It is not limited to small values of shear or of airfoil thickness and it can be used for any profile shape including airfoils with flaps. Comparison between the experimental and theoretical results for the simple nonuniformly sheared flow showed the same type of agreement as is normally obtained in similar comparisons between exact potential flow theory and experiment for uniform flow cases.

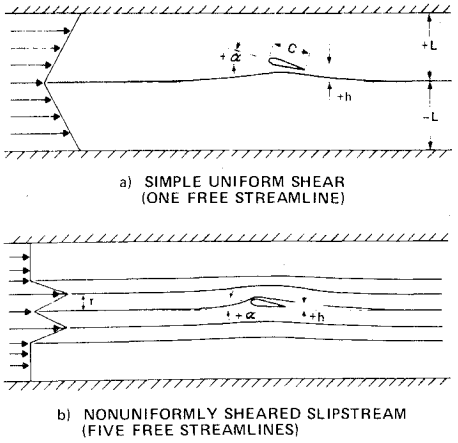

Fig. 1 Schematic of flow models for computer programs.

The investigation reported in this paper continues the line of approach begun in Ref. 5 by extending the theory and the pressure measurements to the nonuniformly sheared slipstream profile of Fig. 1b. In succeeding sections the theoretical approach and its results are described first followed by the experimental approach and its results. Finally, concluding remarks are presented.

Theoretical Investigation

The investigation of Ref. 5 was undertaken to explain the unusual maximum lift and stalling characteristics that had been observed[2] in the two-dimensional flow simulating a nonuniformly sheared slipsteam. The existing theories for airfoils in nonuniformly sheared flows[7-8] were generally limited to small disturbances, i.e., small shear and/or low angles of attack of thin airfoils. It was decided, therefore, to develop a theory, implemented by a digital computer program, which would eliminate these restrictions and be applicable to arbitrary airfoil shapes in large shear at angles of attack near stall. This theory has been described elsewhere.[5,9] A review of its basic features and the extension to the nonuniform slipstream of the present investigation are presented below.

The main characteristic of a sheared flow which distinguishes it from a nonsheared flow is its rotationality. The powerful techniques of potential theory that can be used in two-dimensional uniform flow problems are generally not applicable to rotational flows. The governing equation for the stream function in two-dimensional, incompressible, inviscid shear flow is no longer Laplace's equation, but is

$$\nabla^2\psi = f(\psi) \tag{1}$$

instead. Thus $\nabla^2\psi$ is a constant along each streamline (along which the stream function, ψ, is also a constant). It can be shown that this constant is the vorticity. Except for the case of uniform shear ($f(\psi)$ = const), or the exceptional case $f(\psi) = a\psi$, a = const, Eq. (1) is a nonlinear partial differential equation. However, if the freestream velocity profile can be represented by piecewise linear segments, as in Fig. 1, then regions of constant vorticity are separated by the streamlines that pass through those points at which the velocity gradient changes. This representation reduces the problem of solving a nonlinear partial differential equation with known boundary conditions to a problem with a linear equation ($\nabla^2\psi$ = const)

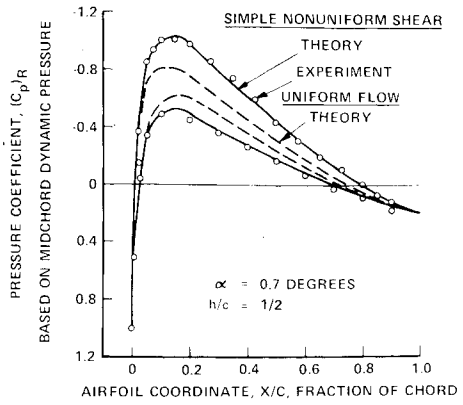

Fig. 2 Comparison of computed and experimental pressure distributions in simple nonuniform shear.

that holds within regions which have free (and, hence, initially unknown) boundaries. It is necessary to adopt an iteration procedure in order to determine the location of these boundaries. In the present theory the free-boundary problem is mechanically implemented for a digital computer in the following way.

The geometrical configurations under consideration are shown in Fig. 1. The airfoil is not limited in thickness and can have an arbitrary profile shape. In the mathematical model the airfoil is represented by a vortex distribution along its actual surface. The wind-tunnel floor and ceiling are incorporated in the model so that the computed results are directly comparable to the experimental ones. These solid boundaries are also represented by surface distributions of vorticity. In its original form,[5] the computer program treated the simple nonuniform shear of Fig. 1a. In this flow the undisturbed velocity distribution is symmetrical above and below the tunnel centerline. Thus, there is a single free streamline which divides regions of vorticity which are of equal magnitude but opposite sign. The extended form of the computer program in the present study treats the nonuniformly sheared slipstream of Fig. 1b with five free streamlines. The undisturbed velocity distribution here is also symmetrical about the centerline. However, the absolute magnitude of the vorticity in the regions near the centerline can be different from that near the outer edges. In principle the two flow problems are the same, but the extra free streamlines complicate the iteration in a practical computational sense.

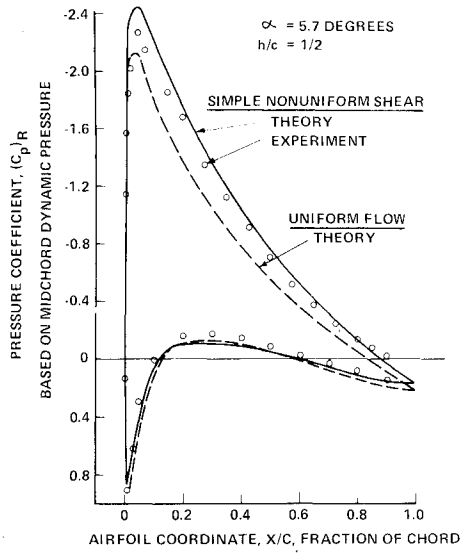

Fig. 3 Comparison of computed and experimental pressure distributions in simple nonuniform shear.

The computation is begun by assuming initial locations of the free streamlines. These should be as close as possible to their final positions, but undistorted straight streamlines are adequate in many cases. With these free streamline boundaries fixed, the vortex distributions representing the airfoil and tunnel boundaries can be found. These distributions are broken up into small segments, each of which has a constant singularity strength. Beyond a specified distance from the airfoil both upstream and downstream, the tunnel boundary vortex distributions are taken to be of constant strength, corresponding to the adjacent undisturbed slipstream velocities. The velocity components induced at any field point by each segment are given by closed form algebraic expressions for the Biot-Savart integrals.[9] Total velocity components due to the tunnel boundaries and the airfoil are then found by summing the contributions of all the segments. To these components are added the contributions induced by the constant vorticity that is distributed over the area between each adjacent pair of free streamlines. Each free streamline is represented in the model by a connected series of straight line segments and the resulting Biot-Savart integrations can again be expressed algebraically and summed over all the regions of the flow. The streamlines are also assumed to be undistorted beyond a specified distance from the airfoil.

The strength of each small vortex segment is found by satisfying the boundary condition of no normal flow across the floor, ceiling, and airfoil surfaces as well as the Kutta-Joukowski condition at the airfoil trailing edge. The normal flow boundary condition is applied at the center of each segment. For N vortex segments, N equations result from the boundary condition and one more from the Kutta-Joukowski condition. Hence a total of $N + 1$ equations is obtained. However, as shown by von Mises,[10] only $N - 1$ of the boundary condition equations are linearly independent and so the set can be made determinate. The resulting set of N linear algebraic equations in N unknown vortex strengths is solved simultaneously using a smoothing technique.[11,12]

The iteration procedure is begun by using these vortex distributions and the flow vorticity to compute velocities from which the mass flow between the tunnel floor and each streamline is determined by integration. This is carried out at each straight line segment that represents the free streamlines. These computed mass flows are compared with their required values which are determined by continuity considerations from the known mass flow between streamlines in the undisturbed slipstream. Corrected streamline locations are then

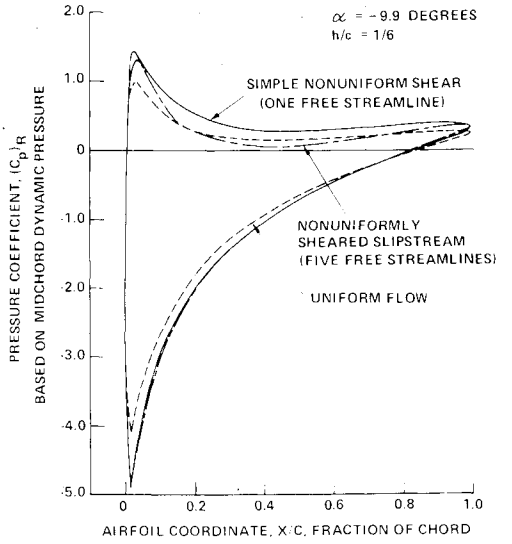

Fig. 4 Comparison of computed pressure distributions in uniform flow, simple nonuniform shear and nonuniformly sheared slipstream.

determined from differences between the computed and required mass flows. Using these corrected streamlines, the airfoil and tunnel boundary vortex distributions can be found again. The iteration process can thus be continued until convergent streamline locations are achieved. Once a convergent solution is obtained in this way, the velocities and pressures anywhere within the field, in particular on the airfoil, can be evaluated.

The validity of this basic theoretical approach can be examined by comparing computed and measured pressure distributions on a symmetrical 17% thickness-to-chord ratio Joukowski airfoil in the simple nonuniform shear of Fig. 1a. Typical comparisons with the airfoil located one-half chord ($h/c = \frac{1}{2}$) above the flow centerline at two angles of attack, α, are given in Fig. 2 for $\alpha = 0.7°$ and in Fig. 3 for $\alpha = 5.7°$. The pressure differences are given in a coefficient form $(C_p)_R$ that is referred to the undisturbed slipstream velocity at the airfoil midchord. The agreement between the theory and experiment is excellent in both examples and is typical of the agreement that is achieved for comparable cases in uniform flow. Figures 2 and 3 also show clearly the significant differences in the pressure distribution between uniform flow and simple nonuniform shear. Although it is not presented here, a similar comparison at $\alpha = 0°$ has the same general features and demonstrates the positive lift that is generated at $\alpha = 0°$ when the airfoil is above the flow centerline. As α approaches stall, however, viscous effects neglected in the theory become more important and the agreement between predicted and measured pressures deteriorates just as it does in uniform flow. Nevertheless, it can be concluded that, in the simple nonuniformly sheared flow, the theoretical approach successfully predicts the important features of the airfoil aerodynamics prior to stall.

Extension of the theoretical approach to the nonuniformly sheared simulated slipstream of Fig. 1b with its five free streamlines is complicated by the necessity to iterate the additional four streamlines. Nevertheless, the five free streamline program has been run to successful convergence for the same airfoil at two different locations in a nonuniformly sheared slipstream. The magnitude of the shear near the center of the slipstream is the same as that used in the previous experimental and theoretical single streamline investigation.[5] Hence, direct comparisons can be made to assess the effects of the slipstream edges. Such a comparison is made in Fig. 4. The computed pressure distributions with the airfoil located one-sixth chord above the flow centerline ($h/c = \frac{1}{6}$), at an angle of attack $\alpha = -9.9°$ are given for the following

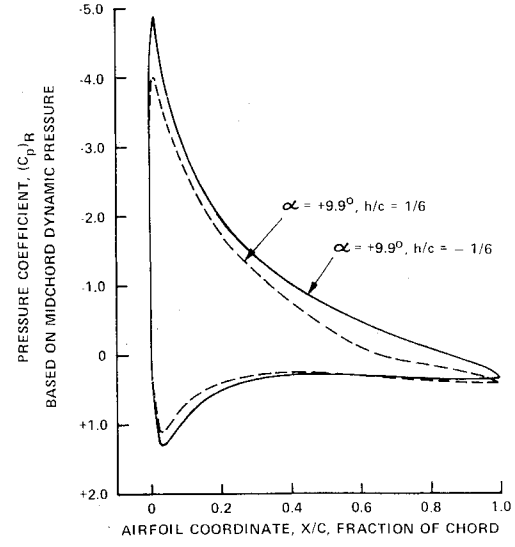

Fig. 5 Comparison of computed pressure distributions on airfoil at two locations in nonuniformly sheared slipstream.

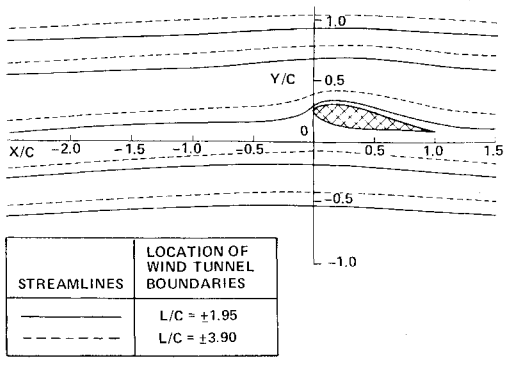

Fig. 6 Free streamline pattern in nonuniformly sheared slipstream for two locations of wind-tunnel floor and ceiling, $h/c = \frac{1}{6}$, $\alpha = 9.9°$.

three cases: uniform flow, simple nonuniform shear and the nonuniformly sheared slipstream. The comparison shows that the simple nonuniform shear and the nonuniformly sheared slipstream generate pressure distributions which differ from that obtained in uniform flow. Inspection of the pressure distributions indicates that for this airfoil location and angle of attack, the two sheared flows should provide almost identical stalling characteristics. However, the lift generated (here of negative sign) in the simple nonuniformly sheared flow will be slightly higher than that generated in the nonuniformly sheared slipstream. On the other hand, the lift generated in the uniform flow will be lower than for both of the other cases. These results are consistent with the available experimental data. Hence, one can conclude that the slipstream edges influence the lift generated in the two nonuniformly sheared flows but should not noticeably change the stalling characteristics if the same shear magnitude is retained. Both the lift and stalling characteristics will differ from those obtained in uniform flow.

The shear used in the above comparison is about one-fifth the magnitude of the shear used in the current experimental program, so that a direct comparison between the five-streamline theory and experiment is not possible at this time. However, the good agreement between theory and experiment obtained with the single free streamline flow illustrates the basic validity of the concepts used for both flow patterns. Moreover, computed pressure distributions such as those illustrated in Fig. 5 for the airfoil located slightly above and slightly below the centerline ($h/c = \pm\frac{1}{6}$) of the moderately sheared nonuniform slipstream show trends which are similar to those observed experimentally in the highly sheared nonuniform slipstream.

The inclusion of the wind-tunnel floor and ceiling in the theoretical model permits a theoretical investigation to determine the effect of these solid boundaries. A limited study was performed wherein the distance L/c between the floor and ceiling for the $h/c = \frac{1}{6}$, $\alpha = 9.9°$ configuration was doubled. The largest effect appears in the locations of the free streamlines for the two cases as shown in Fig. 6. However, the effect on the computed airfoil pressure distributions is not large, see Fig. 7, and the lift is almost identical for the two cases. This indicates that the presence of the wind-tunnel floor and ceiling had only a minor effect on the experiments.

Therefore, although direct comparisons between predicted and measured results have not been possible for the highly sheared slipstream, those theoretical results obtained for moderate shear seem to be in qualitative agreement with the experimental trends. Moreover the theory provides a means of examining parameters such as the amount of shear, the tunnel floor and ceiling locations, and airfoil shape. Such studies could not be carried out easily in the experiments.

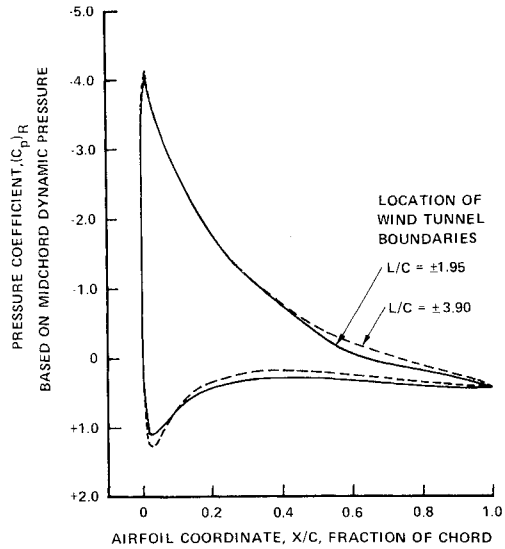

Fig. 7 Computed pressure distributions on airfoil in nonuniformly sheared slipstream for two locations of wind-tunnel floor and ceiling, $h/c = \frac{1}{6}$, $\alpha = 9.9°$.

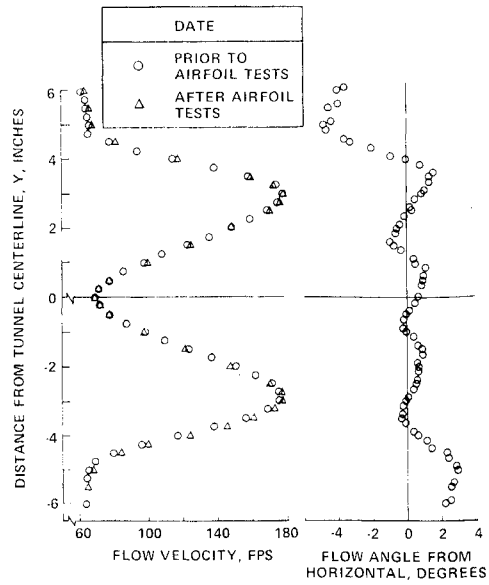

Fig. 9 Measured freestream velocity and angularity distributions at model midchord station in nonuniformly sheared slipstream.

Experimental Investigation

The experimental program consisted of measuring the chordwise pressure distributions on a two-dimensional airfoil located in a nonuniformly sheared flow which simulates a section through a propeller slipstream. The experimental configuration is sketched in Fig. 8. The wind tunnel used is the subsonic leg of the CAL One-Foot High-Speed Wind Tunnel. This leg of the wind tunnel has a test section with a cross section of 17 in. by 24 in. and is operated as a closed-throat nonreturn tunnel. The two-dimensional airfoil used in this research has a symmetric Joukowski profile with a thickness-to-chord ratio of 17% and a chord of 6 in. The airfoil was mounted spanning the wind-tunnel test section. It was supported by a structure which permitted independent change in geometric angle of attack and vertical location.

The sheared flow in the wind-tunnel test section was produced by a screen placed slightly more than 3 ft (between 6 and 7 chords) upstream of the airfoil. This screen consisted of an array of circular rods spanning the wind-tunnel section horizontally and secured by a frame which was clamped between two sections of the wind-tunnel circuit. The spacings between rods and the rod diameters were varied so as to introduce variable losses across the flow. By proper spacing and rod size variation, the vertical distribution of losses in the flow at the screen can be such that the desired sheared flow velocity contour is obtained in the test section. The splitter plates shown in the sketch were inserted to prevent excessive decay of the slipstream before it reached the airfoil location.

Flow velocity in the wind-tunnel test section was measured with a conventional $\frac{3}{16}$-in.-diam pitot-static probe at the axial location of the airfoil midchord. The results are shown in Fig. 9. Two sets of data are shown, one obtained prior to the airfoil pressure tests and one obtained after these tests. As can be seen, the repeatability of the data is excellent. The flow angularity distribution in the slipstream was measured with a crossed hot-wire probe. Initial attempts to obtain a repeatable calibration of a standard yaw probe at various positions in the sheared flow were not successful. However, no difficulties were encountered with the crossed hot-wire. The angularity measurements were made prior to the airfoil pressure tests only and are also shown in Fig. 9. The airfoil geometric angle of attack at each vertical location in the slipstream was corrected to include the measured flow angle at that location.

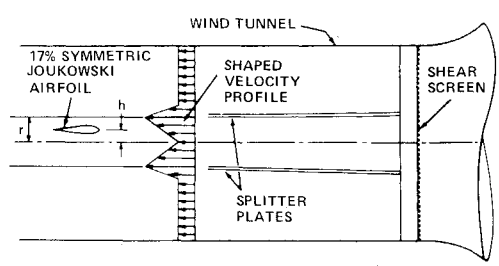

Fig. 8 Sketch of layout for experiments on an airfoil in a two-dimensional highly sheared nonuniform slipstream.

Pressure distributions on the airfoil were obtained through thirty-seven static pressure taps distributed along a chord over the upper and lower airfoil surfaces. These taps were connected to an inclined manometer bank and the resulting pressures were recorded photographically. Pressure distributions were measured over a wide range of angle of attack at each of seven different vertical locations in the slipstream. Separation of the boundary layer on the wind-tunnel walls at the intersection with the airfoil was controlled through the use of sidewall suction. Flow visualization studies using lampblack and kerosene on the wing surface were used to adjust the amount of suction and also as a general tool to study the flow patterns over the wing.

Before considering the pressure distributions, it is of interest to inspect the section lift coefficients obtained by numerical integration of the pressure. Figure 10 shows the section lift coefficients $(C_l)_R$ referenced to the local dynamic pressure in the undisturbed slipstream at the location of the airfoil midchord. This dynamic pressure varies with the vertical position, h/r (see Fig. 8), of the airfoil. These data compare well with balance data obtained previously by Vidal[2] in this same flow. Note the large differences in lift coefficient obtained for airfoil locations slightly above the slipstream centerline ($h/r = +0.158$) and slightly below the slipstream centerline ($h/r = -0.092$). The maximum lift available at these two locations differs by a factor of more than two. Note also the unusual upward curvature of the data for negative airfoil locations and the nonzero lift coefficients for the symmetric airfoil at zero angle of attack. The latter effect is predicted by Tsien's[6] theory for airfoils in uniformly sheared flows and by the present theory for airfoils in nonuniformly sheared flows.

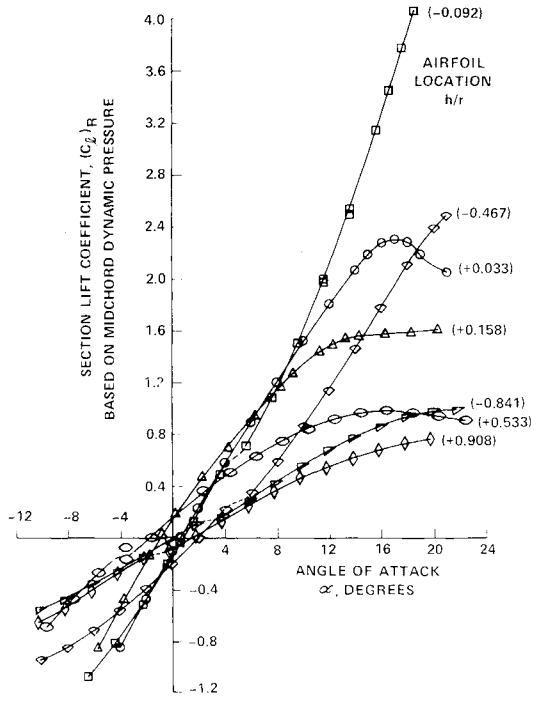

Fig. 10 Section lift coefficient based on midchord dynamic pressure, highly sheared nonuniform slipstream.

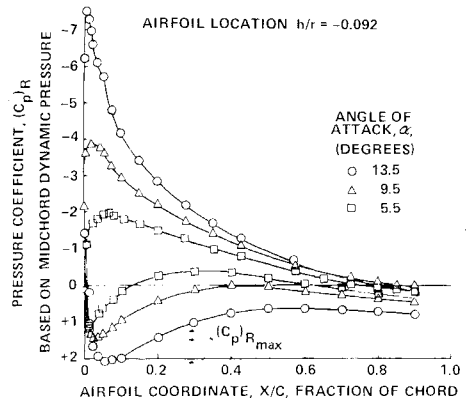

Fig. 11 Experimental pressure distributions on airfoil in two-dimensional, highly sheared nonuniform slipstream.

Sample pressure distributions corresponding to the airfoil location $h/r = -0.092$ are shown in Fig. 11. These pressure coefficients have been referenced to the same local dynamic pressure as the lift coefficients of the previous figure. The most notable feature of these pressure distributions is that the maximum positive pressure coefficient, $(C_p)_{R\,\max}$, differs from a value of unity and varies significantly with angle of attack. For this particular airfoil location, values of $(C_p)_{R\,\max}$ as high as 3 were recorded just before stall. These effects were also obtained at the other airfoil locations in the slipstream and are similar, although substantially greater in magnitude, to those observed in the simple nonuniformly sheared flow experiments.[5] They suggest that a majority of the variation in lift coefficient with airfoil location is due to a change in the stagnation pressure of the streamline which intersects the airfoil (stagnation streamline) as angle of attack is varied. For a given position of the airfoil midchord, a change in angle of attack changes the circulation about the airfoil and, hence, changes the position in the flow upstream from which the stagnation streamline originated. Of course the same is true for an airfoil in uniform flow. However, the change in upstream position of the stagnation streamline in a sheared flow results in a change in stagnation pressure of the flow which encounters the airfoil as the airfoil's angle of attack is varied. Since the lift on the airfoil is a function of the stagnation pressure of the flow as well as the angle of attack, the variation of lift with angle of attack in a sheared flow will be different from that in a uniform flow.

The dynamic pressure associated with the stagnation streamline is given by the pressure at the positive pressure peak on the airfoil. Hence, it should be possible to reduce the variations in the lift data by using this stagnation pressure as a reference dynamic pressure to compute lift coefficients. This has been done for the lift coefficient data shown previously (Fig. 10), and the results are plotted in Fig. 12 for three airfoil locations near the slipstream centerline. The angle of attack for zero lift has been subtracted from the usual angle of attack in this figure in order to facilitate direct comparison of the shapes of the lift coefficient curves.

One can conclude from the very much smaller differences in Fig. 12 that the displacement of the stagnation streamline with changes in angle of attack is largely responsible for the unusual lift behavior found originally by Vidal[2] for airfoil locations near the slipstream centerline. This finding is in agreement with the work[5] on the simple nonuniformly sheared flow. For airfoil locations farther removed from the slipstream centerline, this method of data reduction considerably reduced the differences between the lift curves for the various airfoil locations. However, the degree of correlation is not as high as that obtained for the airfoil located near the centerline. It would appear that proximity of the airfoil to the slipstream edges has an effect on the lift which is not completely explained by the stagnation streamline argument. Inspection of the theoretical pressure distributions shown in Fig. 4 leads to a similar conclusion.

The region of greatest interest is the one in which the airfoil is located near the slipstream centerline. It is in this region that a change in the vertical location of the airfoil of less than one airfoil thickness produced a more than twofold change in maximum lift available. Flow visualization studies with lampblack and kerosene showed that the airfoil began to stall near the trailing edge at angles of attack as low as nine degrees for $h/r = +0.158$, whereas for $h/r = -0.092$, stall did not occur until an angle of attack larger than eighteen degrees was reached. Several pressure distributions for these two airfoil locations are shown in Fig. 13 along with an indication of the boundary-layer separation points observed visually and those estimated theoretically. The theoretical method for calculating the separation point follows the work of Sandborn and Liu.[13] The particular form of the separation criterion is shown on Fig. 13. This form appeared to give the best engineering estimate of the separation point using the experimental pressure distributions obtained on the airfoil both in uniform flow and in the sheared slipstream. Note that separation is neither observed nor predicted for the pressure

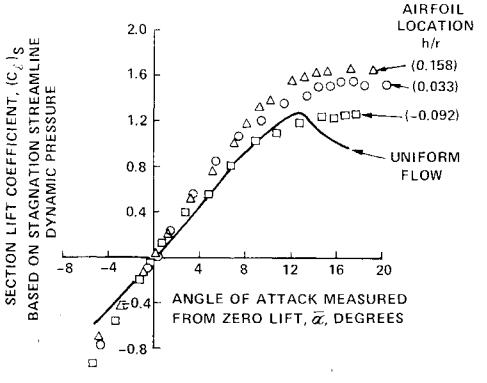

Fig. 12 Section lift coefficient based on stagnation streamline dynamic pressure, highly sheared nonuniform slipstream.

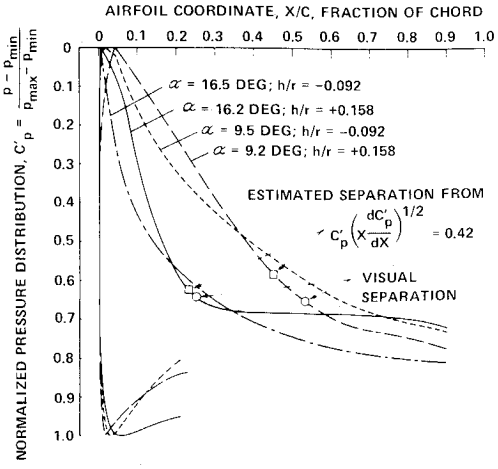

Fig. 13 Comparison of experimental pressure distributions for airfoil locations near centerline of highly sheared nonuniform slipstream.

distribution measured on the airfoil located at $h/r = -0.092$, even at an angle of attack of 16.5°.

These results suggest that the unusual airfoil stalling characteristics are due simply to the differences in the upper surface pressure distributions. These pressure distributions in turn depend on the freestream shear and the location of the airfoil in the sheared flow. It does not appear to be necessary to consider the direct action of the freestream shear on the boundary-layer separation point other than the way in which the shear influences the pressure. Hence, this work confirms the suggestion put forth earlier[5] that if the pressure distribution on a wing in an inviscid sheared flow is predictable, then the techniques which are used to predict stalling characteristics of airfoils in uniform flow from inviscid pressure distributions should also be applicable here.

As a final observation on the experimental results, it is perhaps worth mentioning that the combined results of the current work and that performed earlier in the simple nonuniform shear[5] show that no generalization can be made regarding the effect of airfoil location in a sheared flow on the stalling characteristics of the airfoil. In the earlier work[5] it was found that a location of the airfoil above the flow centerline (positive shear) delayed separation while the converse was true for locations below the flow centerline (negative shear). In the current work, separation was greatly delayed at an airfoil position just below the flow centerline and was promoted at an airfoil position just above the centerline. Apparently, it is necessary to examine pressure distributions for each case before stalling characteristics can be estimated.

Conclusions

The experimental research on airfoils in two-dimensional sheared flows has shown that such flows can have very large effects on airfoil lift and stalling characteristics. The effects on lift which occur prior to stall appear to be predictable by the inviscid theory which has been developed. The experimental studies have shown that airfoil stalling characteristics in a sheared flow are governed by the shear-dependent upper surface pressure distributions. However, it is not possible at this time to arrive at generalizations relating airfoil stalling characteristics to airfoil location in sheared flows. Nevertheless, since the theory provides the inviscid pressure distributions on the airfoil, it should be possible to use these distributions to estimate stalling characteristics in those situations where converged solutions can be obtained. Though only a limited number of converged solutions have been obtained at the present time, it is believed that further development of the theoretical model and its implementation on the computer would allow investigation of a wide variety of airfoils in sheared flow configurations of practical interest.

References

[1] Sowyrda, A., "Theory of Cambered Joukowski Airfoils in Shear Flow," Rept. AI-1190-A-2, Sept. 1958, Cornell Aeronautical Lab. Inc., Buffalo, N.Y.

[2] Vidal, R. J., "The Influence of Two-Dimensional Stream Shear on Airfoil Maximum Lift," *Journal of the Aerospace Sciences*, Vol. 29, No. 8, Aug. 1962, pp. 889–904.

[3] Vidal, R. J. and Curtis, J. T., "The Effects of Axisymmetric Shear on Airfoil Characteristics," TR 61-138, Dec. 1961, U.S. Army Transportation Research Command, Fort Eustis, Va.

[4] Brady, W. G., "Theoretical and Experimental Studies of Airfoil Characteristics in Nonuniform Sheared Flow," TR 65-17, May 1965, U.S. Army Aviation Materiel Labs., Fort Eustis, Va.

[5] Brady, W. G. and Ludwig, G. R., "Aerodynamic Properties of Airfoils in Nonuniformly Sheared Flows," *Proceedings of the CAL/USAAVLABS Symposium on Aerodynamic Problems Associated with V/STOL Aircraft*, Vol. 2, Technical Session 4, June 1966, Cornell Aeronautical Lab. Inc., Buffalo, N.Y.

[6] Tsien, H. S., "Symmetric Joukowski Airfoils in Shear Flow," *Quarterly of Applied Mathematics*, Vol. 1, No. 2, July 1943, pp. 130–148.

[7] Jones, E. E., "The Forces on a Thin Airfoil in Slightly Parabolic Shear Flow," *Zeitschrift fur Angewandte Mathematik und Mechanik*, Vol. 37, No. 9/10, Sept.-Oct. 1957, pp. 362–370.

[8] Jones, E. E., "The Elliptic Cylinder in a Shear Flow with Hyperbolic Velocity Profile," *Quarterly Journal of Mechanics and Applied Mathematics*, Vol. 12, Pt. 2, May 1959, pp. 191–210.

[9] Brady, W. G. and Ludwig, G. R., "Theoretical and Experimental Investigation of the Aerodynamic Properties of Airfoils Near Stall in a Two-Dimensional Nonuniformly Sheared Flow," TR 66-36, June 1966, U.S. Army Aviation Materiel Labs., Fort Eustis, Va.

[10] von Mises, R., *Theory of Flight*, McGraw-Hill, New York, 1945, pp. 188–198.

[11] Phillips, B. L., "A Technique for the Numerical Solution of Certain Integral Equations of the First Kind," *Journal of the Association for Computing Machinery*, Vol. 9, No. 1, Jan. 1962, pp. 84–97.

[12] Twomey, S., "On the Numerical Solution of Fredholm Integral Equations of the First Kind by the Inversion of the Linear System Produced by Quadrature," *Journal of the Association of Computing Machinery*, Vol. 10, No. 1, Jan. 1963, pp. 97–101.

[13] Sandborn, V. A. and Liu, C. Y., "On Turbulent Boundary-Layer Separation," *Journal of Fluid Mechanics*, Vol. 32, Pt. 2, May 1968, pp. 293–304.